ANALYSIS OF ACTIVE LAYER THICKNESS ON THIN LAYER SOLAR CELL PERFORMANCE

Soni Prayogi[1,2*], D. Darminto[2]

[1]Department of Electrical Engineering, Faculty of Industrial Technology, Pertamina University, Jl. Teuku Nyak Arief, Jakarta, 12220, Indonesia.
[2]Department of Physics, Faculty of Science and Data Analytics, Institut Teknologi Sepuluh Nopember, Jl. Teknik Kimia, Surabaya, 60111, Indonesia.

Received: 30th November 2022; Revised: 5th April 2023; Accepted: 12th April 2023

ABSTRACT

The main objective of this research is to fabricate double-layer hydrogenated amorphous silicon (a-Si:H) using a PECVD by varying the thickness of the active layer. To obtain the thickness of the double active layer, dilution of silane plasma is carried out by hydrogen, with a ratio of hydrogen and silane, $R=H_2/SiH_4$ varies, and the deposition time of the active layer, while the n-type and n-type extrinsic layers are fixed for each -each sample. Then on the sample, there is a metal coating on the back which acts as an electrical contact and light reflector. Additionally, each sample was examined or searched for with a sun simulator and sunlight for physical properties, such as thickness morphology, optical properties, such as bandgap, electrical properties, such as electrical conductivity, and I-V characterization of a-Si: H double active layer solar cells. Based on the I-V characterization of the a-Si: H double active layer solar cells that were found in this work, a satisfactory conversion efficiency (8.86%) was found, although the Field Factor of the active layer was still low. While the intrinsic photo response reached 10^5

Keywords: a-Si: H; PECVD; efficiency

Introduction

Amorphous silicon (a-Si:H), microcrystalline silicon (c-Si), and polycrystalline silicon are all often produced using the original approach of adding hydrogen into the materials (poly-Si).[1] Solar cells currently use a-Si H-based thin film semiconductors.[2] Technology era, a-Si: H thin films may be produced using a variety of deposition techniques. Only PECVD (plasma-enhanced chemical vapor deposition) has been developed for industrial use.[3] However, the rate of deposition of device-quality a-Si: H films produced by PECVD at the standard frequency of 13.56 MHz with the best deposition settings is low.[4] A low deposition rate is associated with lengthy processing periods and expensive manufacturing costs.[5] For industrial applications, high deposition rates of device-quality films with optical and electrical properties are required.[6] The result is the use of high power, high pressure, and high plasma excitation frequency.[7]

The device-grade silicon layers of silicon-based solar cells are typically deposited at 300 °C.[8] In addition, the use of inexpensive substrates is made possible by lowering the production temperature, which also has economic benefits by reducing the energy needed to produce the devices.[9] Although the quality of the films deposited at low temperatures can be enhanced by adjusting the deposition parameters, such as the RF power and hydrogen dilution in SiH_4 by the RF-PECVD technique, it is observed that films deposited at low Ts are frequently porous and more disordered, and they have poor optoelectronic properties.[10] The concentration of different radicals in the plasma is governed by growth parameters such SiH4 flow rate, RF power, and process pressure.[11] Additionally, H_2/SiH_4 is the main factor that determines the density of atomic hydrogen in plasma.[12] The

*Corresponding author.
E-Mail: prayogi.sp@gmail.com

weak Si-Si connections are broken by the atomic hydrogen that comes to the surface of the expanding films during etching, and the stronger Si-Si bonds are created in their stead.[13] Moreover, the film may be penetrated by atomic hydrogen, which might alter the bonding and promote the formation of more ordered a-Si: H films.[14]

Here, we describe a unique method for producing active layers of amorphous silicon structures from SiH_4 using the RF-PECVD process. We also evaluate the effectiveness of the method by varying the thickness of each active layer via the deposition period.

Methods

Using the RF-PECVD technique, the active layer a-Si: H solar cell deposition was completed. To obtain the active layer, dilution of silane plasma by hydrogen was carried out, with a varying ratio of hydrogen and silane, $R=H_2/SiH_4$. To create a thin film that can absorb the widest range of solar radiation, the active layer a-Si: H solar cell structure, as illustrated in Figure 1, will be formed using typical deposition settings. Moreover, it is anticipated that the stated deposition conditions would result in higher-quality solar cells.

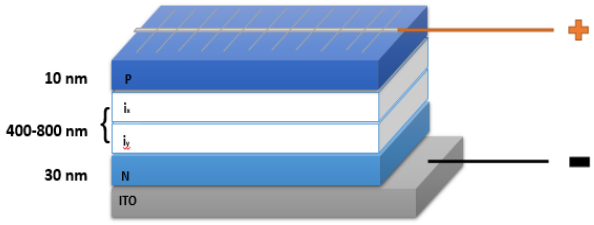

Figure 1. Schematic design of a-Si: H-based active layer solar cells

Various characterization techniques will be used to determine the quality (optimization) of the resulting a-Si: H active layer solar cells, including surface morphology. Characterization of solar cells using AFM, electrical conductivity, absorption, transmittance, and energy gap measurements, as well as I-V characterisation (Sun Solarimeter and Sunlight).

The following processes are used to process and analyze the measurement data of the typical solar cell properties under irradiation circumstances: 1) Plot the solar cell's characteristic current-voltage (I-V) curve using the measurement data. 2) Determine V_{oc}, I_{sc}, and V_mI_m from the I-V characteristic curve. The ammeter displays the I_{sc} value, and the voltage displayed on the voltmeter is zero when the variable resistor is at zero. When the value of the resistor rises, the amount of the current reduces, causing the voltage to gradually climb. The magnitude of the current is zero and the voltage approaches the value V_{oc} up until the resistor reaches a value that is almost infinity. While V_m and I_m respectively are the voltage and current at the optimum operating point. 3) Determine the fill factor (FF) and efficiency (η) of the solar cell.[15] A dimensionless number called FF expresses the proportion of a solar cell's maximum power to its multiplication of I_{sc} and V_{oc}.

Result and Discussion

The RF-PECVD technique was used to deposit the active layer of the a-Si: H solar cell. While the n-type and n-type extrinsic layers are constant for each sample, the double intrinsic layer is created by hydrogen dilution of silane plasma with variable hydrogen to silane ratio, $R=H_2/SiH_4$.

According to the photograph of each sample in the attachment, the intended outcome of this experiment is a uniform coating of a blue-black hue. As a result of the layer's uniform blue-black tint, it is regarded as homogenous. The stages of deposition can be used to explain the results of the experiment's deposition of a-Si: H layers; specifically, the second type of deposition results can be explained by the likelihood that dust (dust) will occur during the second stage of deposition. Dust creates significant cavities on the surface.[16] The second sample image demonstrates that a significant quantity of empty space (voids) is created when the dust reaches the surface because it is unable to move freely.

 ISSN:1979-6374/ EISSN:2460-5999

Due to this, the second type appears as blank spaces (voids). The likelihood of the second type of deposition results forming because of this incidence is very high. The third step of the deposition procedure is highly likely to produce the outcome of the third type of deposition. Cross-links form in the third stage of the second reaction equation after the Si-H clusters have diffused, trapping the H_2 molecules in the layer. High stresses and strains result in a fragile surface in the final step. Surface weak connections are quickly disrupted when activation energy is present. H atoms will be released into the outside air because of the broken links between Si. Such occurrences can be seen in the third category of deposition outcomes. The a-Si: H layer eventually separates from the substrate as shown in the third sample image once the deposition is finished, happening like a branch that keeps growing.[17]

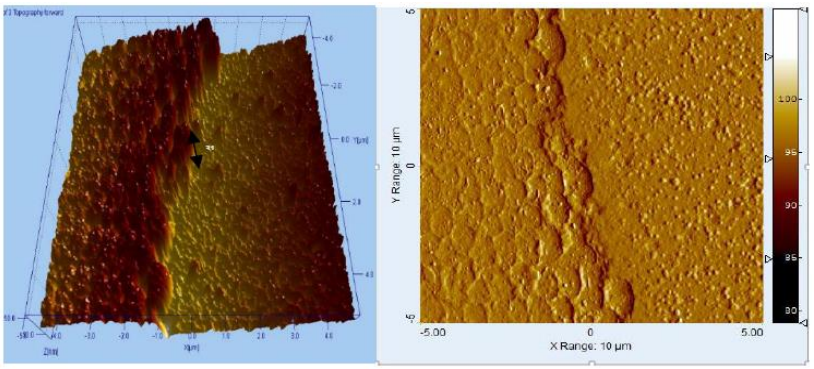

(a)

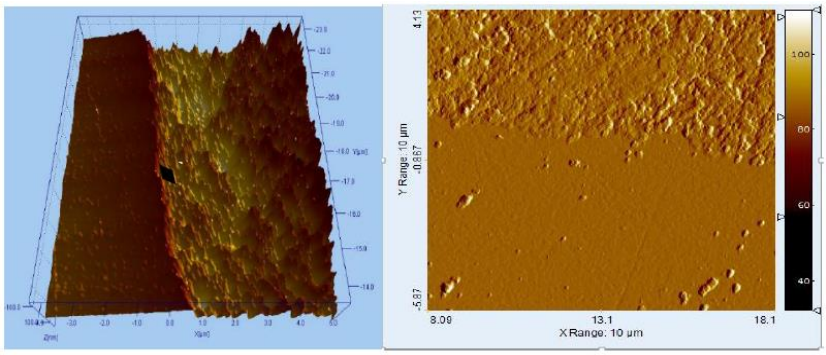

(b)

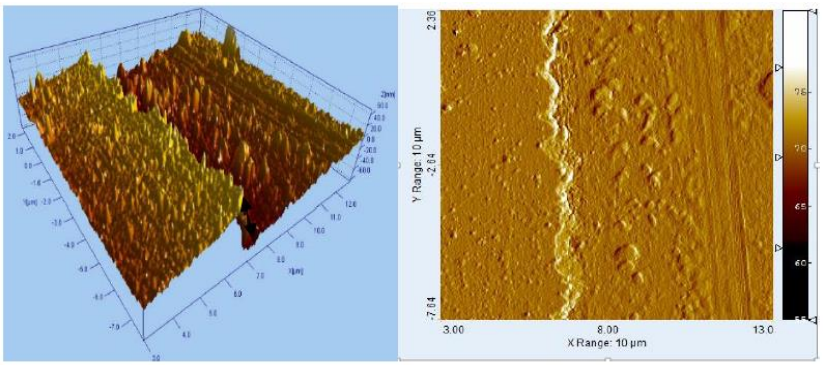

Figure 2. Surface morphology of the active layer as measured using AFM (a) Active layer 1, (b) Active layer 2, and (c) Active layer 3.

The thickness and morphology of the sample may be measured using atomic force microscopy (AFM), which analyzes the material utilizing atomic forces between the tip and the substrate. AFM includes several components: tips, cantilevers, piezoelectric sensors, and photodetectors. The cantilever slope changes as the tip moves across the test material's surface throughout the material characterization procedure. The photodetector picks up the cantilever's tilt.[18] The detector receives the laser beam that was directed at the cantilever, which is then used to detect the cantilever's tilt. At the boundary between the coating and the substrate, measurements or scanning are obtained (no coating).

Information about depth is provided by the slope change. Scanning in this border region yielded data on height or depth variations that represented the thin layer's thickness. Figure 2 shows the outcomes of measurements made using AFM for every active layer.

The sample's energy gap (E_g) can be calculated by measuring the conductivity of the sample at each temperature rise (T), which results in a graph of ln vs 1/T. It is also feasible to calculate the energy gap of the sample by measuring the conductivity at different temperatures.(19) The graph's slope can be used to establish where the E_g is located as shown in Figure 1. According to the findings of UV-Vis's measurements and analysis using Tauc's Plot method and a ratio of ln to 1/T, each layer has successfully optimized the energy gap (Eg) in the active layer a-Si: H solar cell samples.

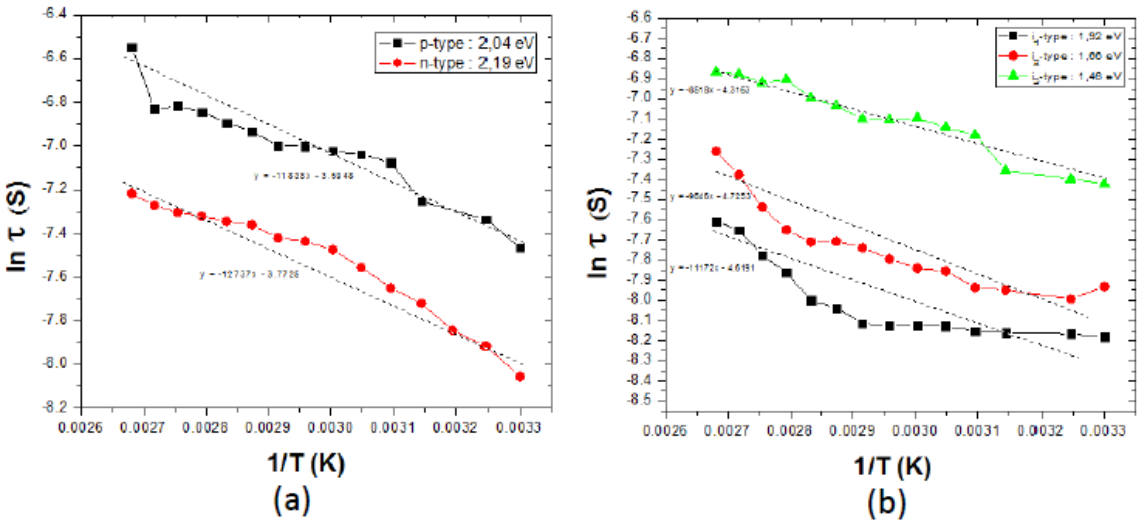

Figure 3. Measurement of E_g using the ratio of ln σ to 1/T (a). The active layer, and (b). Passive layer.

The test sample is trimmed to a size of 1 x 1 cm^2 for the four-point method of measuring electrical conductivity. With the intention of lowering the measurement correction factor, the sample area is made as small as possible. The form of the sample will have an impact on the measurement correction factor in addition to ensuring that the sample size is as little as possible.[20] The measurement correction factor must also be taken into consideration if the sample shape is circular.[21] As a result, rather than employing a circle as the sample form for the four-point probe measurement of electrical conductivity, a square 1x1 cm^2 in size is used. The probes are spaced 0.25 cm apart because the sample is 1x1 cm^2.

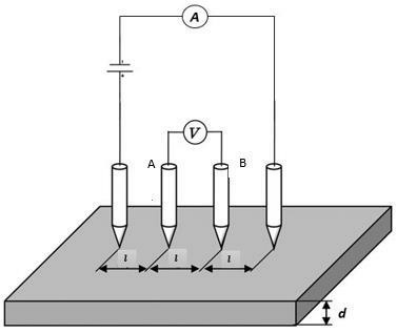

Figure 4. Schematic of the conductivity measurement circuit using the four-point method

The conductivity value is obtained from the equation above. From this equation, it can be concluded that the magnitude of the electrical conductivity value of a sample is influenced by several variables. Among them is the voltage, the thickness of the coating, the distance between the probes, and the current that is read.[22] With the flow of electric current on the two outermost probes, a Voltage value (V) will be obtained from the measured voltage value on the two innermost probes.

Table 1. Results of electrical conductivity studies under light circumstances of the intrinsic and extrinsic layers

No	Sample	Voltage V_{a-b} (V)	Current I (mA)	Conductivity σ (x10^{-3} S/cm)
1	Tipe-p	0,647	96,2	1,74
2	Tipe-n	0,461	64,3	3,15
3	Tipe-i_1	0,847	277,2	65,1
4	Tipe-i_2	0,747	176,2	35,4
5	Tipe-i_3	0,844	246,2	60,6

Table 2. Results of electrical conductivity tests performed in the dark on the intrinsic and extrinsic layers

No	Sample	Voltage V_{a-b} (V)	Current I (mA)	Conductivity σ (x10^{-3} S/cm)
1	Tipe-p	0,325	36,2	0,48
2	Tipe-n	0,231	64,3	0,85
3	Tipe-i_1	0,627	147,2	0,62
4	Tipe-i_2	0,541	106,1	0,31
5	Tipe-i_3	0,642	142,7	0,56

The active layer a-Si: H in the solar cell device layer plays a critical role in using photon energy to excite its charge carriers from the valence band to the conduction band and to strengthen the electric field between the p-layer and n-layer.[23] The rate of charge carrier production will accelerate with increasing active layer thickness, and photon absorption will be greater.[24] The series resistance (Rs), however, also rises because of localized circumstances brought on by the thicker i-layer. On the other hand, if the i-layer is too thin, the electric field that is formed between the p-layer and n-layer would diminish.

Tables 1 and 2 show that the conductivity of the light is not noticeably higher in the extrinsic layer than it is in the dark condition. The photo response (σ_{ph}/σ_{pd}), the extrinsic layer is a passive layer if it has a value of 10^1 or less for the ratio of light conductivity to dark conductivity. This is due to the fact that the concentration of electrons in the conduction band does not appreciably increase as a result of the electrons moving from the valence band that is stimulated by light towards the conduction band.[25] The

 ISSN:1979-6374/ EISSN:2460-5999

excited electrons greatly increase the concentration of electrons in the conduction band in comparison to the active layer, which has a photosensitivity of up to 10^5 As a result, it is noticed that the conductivity of light on the intrinsic type seems to rise dramatically.[26]

Measurement of I-V with Sun Simulator for the characteristics of active layer a-Si: H solar cells. The Sun Simulator is made of aluminum with a size of (15x15x30) cm^3 and is connected to an electronic circuit. At the top is placed a lamp to measure the I-V characteristics in irradiated conditions. The lamp used is a Halogen Bulb lamp with a light intensity of 46.6 mW/cm^2. Halogen Bulm lamps were chosen because their light spectrum is almost close to the spectrum of sunlight.

The I-V characterization process with direct sunlight is, in principle, almost the same as using the Sun Simulator, but the fundamental difference is that the light source is through direct sunlight where the light intensity reaches 850 mW/cm^2. The I-V characterization procedure for this solar cell was carried out three times according to the number of samples.

Optimization results are carried out through differences in the thickness of the active layer. The results of the active layer I-V characterization with differences in layer thickness with the Sun Simulator and sunlight can be seen in Table 3 and Table 4.

Table 3. I-V characterization of active layer a-Si: H solar cells with different layer thicknesses using the Sun Simulator

No	Thickness	V_{oc} (mV)	I_{sc} (mA)	P_{in} (mW)	P_{maks} (mW)	*FF*	H (%)
1	$i_1 < i_3$	164,4	0,282	366	29,18	0,62	7,97
2	$i_1 = i_3$	178,2	0,288	366	31,05	0,57	8,48
3	$i_1 > i_3$	182,1	0,298	366	32,45	0,58	8,86

Table 3. I-V characterization of active layer a-Si: H solar cells with different layer thicknesses using the Sunlight

No	Thickness	V_{oc} (mV)	I_{sc} (mA)	P_{in} (mW)	P_{maks} (mW)	*FF*	H (%)
1	$i_1 < i_3$	341,20	0,529	1144	89,14	0,49	7,79
2	$i_1 = i_3$	374,60	0,586	1144	92,49	0,42	8,25
3	$i_1 > i_3$	381,50	0,591	1144	97,18	0,43	8,49

Using the Sun Simulator and direct sunlight, researchers were able to characterize the active layer of an a-Si: H solar cell from an I-V perspective. The findings revealed that the measurements obtained varied in the i-thickness layer's between 400 and 800 nm. In the results of previous studies using the same PECVD tool with a p-i-n structure, it produced an efficiency of 5.31%. Meanwhile, by optimizing by varying the energy gap and

 ISSN:1979-6374/ EISSN:2460-5999

the thickness of each sample, the efficiency value is 8.86%. There was a very significant increase in efficiency, almost 70% from what had been done before.

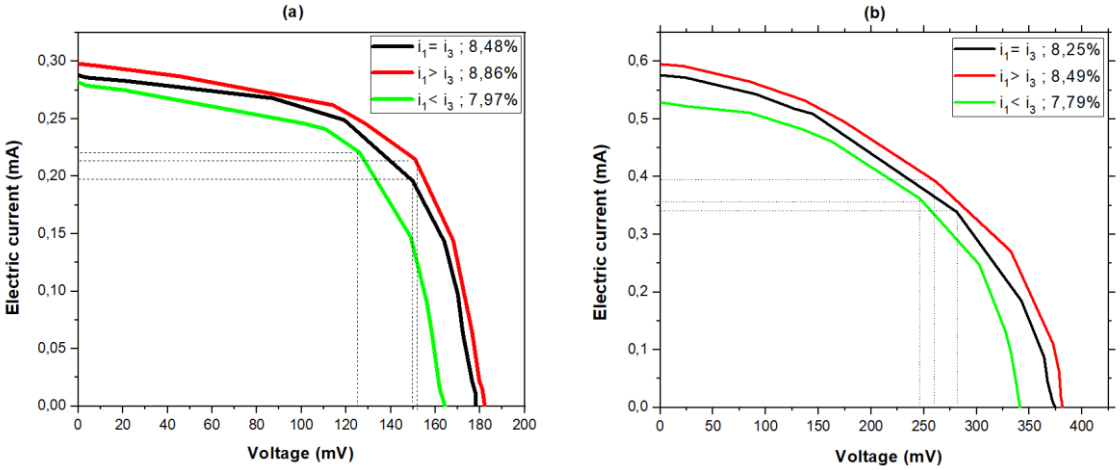

Figure 5. Graph of Sample Efficiency based on differences in intrinsic layer thickness measurements with (a) Sun Simulator, and (b) Sunlight

Overall, as evidenced by low maximum output power, the resulting a-Si: H active layer solar cells typically have a poor FF. One of the causes of the active layer a-Si: H solar cells' low FF value is the imperfect junction creation mechanism, which results in flaws in the interface area. The resultant a-Si: H solar cell has five junction points, each of which is a junction between the substrate (ITO) and the p-layer, between the p-layer and the p-layer, and between the p-layer and the p-layer. Defective conditions will be created in the joint area if the connecting mechanism between the layers is improperly built.

The important role of the active layer a-Si: H in the solar cell device layer is to employ photon energy to excite its charge carriers from the valence band to the conduction band and to strengthen the electric field between the p-layer and n-layer. More photon absorption will result from a larger active layer since charge carrier generation will occur more quickly.[27] However, the series resistance (Rs) also rises because of localized circumstances brought on by the thicker i-layer. The electric field that is created between the p-layer and n-layer will weaken if the i-layer is too thin, on the other hand.

Conclusion

In summary, from the measurements of the electrical conductivity of each sample, the photo response (σ_{ph}/σ_{pd}) the extrinsic layer exhibits a value of no more than 10^1 for the ratio of light conductivity to dark conductivity, whereas the photo response (σ_{ph}/σ_{pd}) of the intrinsic can reach 10^5. As a result, it may be inferred that the intrinsic layer is active, and the extrinsic layer is inactive. An excellent conversion efficiency (8.86%) was obtained based on the I-V characterization of the a-Si: H active layer solar cell found in this work. However, the I-V characteristics of the active layer a-Si: H solar cells produced in this study still show a low fill factor (FF). The most likely cause of the low fill factor (FF) value is the connection mechanism in the areas between layers (interface) which is not yet perfect, thus creating defective conditions in these areas.

Acknowledgment

The author would like to thank Institut Teknologi Sepuluh Nopember and Pertamina University for its support.

References

1. Guha S. Amorphous Semiconductor Solar Cells. In: Buschow KHJ, Cahn RW, Flemings MC, Ilschner B, Kramer EJ, Mahajan S, et al., editors. Encyclopedia of Materials: Science and Technology [Internet]. Oxford: Elsevier; 2001 [cited 2022 Nov 20]. p. 259–63. Available from:

https://www.sciencedirect.com/science/article/pii/B0080431526000565
2. Kasap S, Koughia C, Singh J, Ruda H, O'Leary S. Optical Properties of Electronic Materials: Fundamentals and Characterization. In: Kasap S, Capper P, editors. Springer Handbook of Electronic and Photonic Materials [Internet]. Boston, MA: Springer US; 2007 [cited 2022 Nov 2]. p. 47–77. (Springer Handbooks). Available from: https://doi.org/10.1007/978-0-387-29185-7_3
3. Flewitt AJ. Hydrogenated Amorphous Silicon Thin-Film Transistors (a-Si:H TFTs). In: Chen J, Cranton W, Fihn M, editors. Handbook of Visual Display Technology [Internet]. Cham: Springer International Publishing; 2016 [cited 2022 Nov 20]. p. 887–909. Available from: https://doi.org/10.1007/978-3-319-14346-0_47
4. Prayogi S, Cahyono Y, Darminto D. Electronic structure analysis of a-Si: H p-i1-i2-n solar cells using ellipsometry spectroscopy. Opt Quantum Electron. 2022 Sep 16;54(11):732.
5. Illiberi A, Kudlacek P, Smets AHM, Creatore M, van de Sanden MCM. Effect of ion bombardment on the a-Si:H based surface passivation of c-Si surfaces. Appl Phys Lett. 2011 Jun 13;98(24):242115.
6. Rozati SM, Ziabari SAM. A review of various single layer, bilayer, and multilayer TCO materials and their applications. Mater Chem Phys. 2022 Dec 1;292:126789.
7. Wang SH, Chang HE, Lee CC, Fuh YK, Li TT. Evolution of a-Si:H to nc-Si:H transition of hydrogenated silicon films deposited by trichlorosilane using principle component analysis of optical emission spectroscopy. Mater Chem Phys. 2020 Jan 15;240:122186.
8. Duan W, Qiu Y, Zhang L, Yu J, Bian J, Liu Z. Influence of precursor a-Si:H dehydrogenation on the aluminum induced crystallization process. Mater Chem Phys. 2014 Jul 15;146(1):141–5.
9. Morigaki K, Ogihara C. Amorphous Semiconductors: Structure, Optical, and Electrical Properties. In: Kasap S, Capper P, editors. Springer Handbook of Electronic and Photonic Materials [Internet]. Boston, MA: Springer US; 2007 [cited 2022 Nov 20]. p. 565–80. (Springer Handbooks). Available from: https://doi.org/10.1007/978-0-387-29185-7_25
10. Hamdani D, Prayogi S, Cahyono Y, Yudoyono G, Darminto D. The influences of the front work function and intrinsic bilayer (i1, i2) on p-i-n based amorphous silicon solar cell's performances: A numerical study. Cogent Eng. 2022 Dec 31;9(1):2110726.
11. Prayogi S, Ayunis, Kresna, Cahyono Y, Akidah, Darminto. Analysis of thin layer optical properties of A-Si:H P-Type doping CH$\less$sub$\greater$4$\less$/sub$\greater$ and P-Type without CH$\less$sub$\greater$4$\less$/sub$\greater$ is deposited PECVD systems. J Phys Conf Ser. 2017 May;853:012032.
12. Camargo SS, Carreño MNP, Pereyra I. Hydrogen effusion from highly-ordered near-stoichiometric a-SiC:H. J Non-Cryst Solids. 2004 Jun 15;338–340:70–5.
13. Sriraman S, Agarwal S, Aydil ES, Maroudas D. Mechanism of hydrogen-induced crystallization of amorphous silicon. Nature. 2002 Jul;418(6893):62–5.
14. Prayogi S, Cahyono Y, Hamdani D, Darminto. Effect of active layer thickness on the performance of amorphous hydrogenated silicon solar cells. Eng Appl Sci Res. 2022;49(2):201–8.
15. Irvine S. Solar Cells and Photovoltaics. In: Kasap S, Capper P, editors. Springer Handbook of Electronic and Photonic Materials [Internet]. Boston, MA: Springer US; 2007 [cited 2022 Nov 16]. p. 1095–106. (Springer Handbooks). Available from: https://doi.org/10.1007/978-0-387-29185-7_46

16. Pedrak R, Ivanov Tzv, Ivanova K, Gotszalk T, Abedinov N, Rangelow IW, et al. Micromachined atomic force microscopy sensor with integrated piezoresistive sensor and thermal bimorph actuator for high-speed tapping-mode atomic force microscopy phase-imaging in higher eigenmodes. J Vac Sci Technol B Microelectron Nanometer Struct Process Meas Phenom. 2003 Nov;21(6):3102–7.
17. Dzedzickis A, Bucinskas V, Viržonis D, Sesok N, Ulcinas A, Iljin I, et al. Modification of the AFM Sensor by a Precisely Regulated Air Stream to Increase Imaging Speed and Accuracy in the Contact Mode. Sensors. 2018 Aug;18(8):2694.
18. Xu Y, Yan XT, editors. Thermodynamics and Kinetics of Chemical Vapour Deposition. In: Chemical Vapour Deposition: An Integrated Engineering Design for Advanced Materials [Internet]. London: Springer; 2010 [cited 2022 Nov 16]. p. 129–64. (Engineering Materials and Processes). Available from: https://doi.org/10.1007/978-1-84882-894-0_4
19. Prayogi S, Cahyono Y, Darminto. Fabrication of solar cells based on a-Si: H layer of intrinsic double (P-i $\less$sub$\greater$x$\less$/sub$\greater$ -i $\less$sub$\greater$y$\less$/sub$\greater$ -N) with PECVD and Efficiency analysis. J Phys Conf Ser. 2021 Jun;1951(1):012015.
20. Hamdani D, Prayogi S, Cahyono Y, Yudoyono G, Darminto D. The Effects of Dopant Concentration on the Performances of the a-SiOx:H(p)/a-Si:H(i1)/a-Si:H(i2)/µc-Si:H(n) Heterojunction Solar Cell. Int J Renew Energy Dev. 2022 Feb 1;11(1):173–81.
21. Meng F, Shen L, Shi J, Zhang L, Liu J, Liu Y, et al. Role of the buffer at the interface of intrinsic a-Si:H and p-type a-Si:H on amorphous/crystalline silicon heterojunction solar cells. Appl Phys Lett. 2015 Nov 30;107(22):223901.
22. Prior KA. SEMICONDUCTOR PHYSICS | Impurities and Defects. In: Guenther RD, editor. Encyclopedia of Modern Optics [Internet]. Oxford: Elsevier; 2005 [cited 2022 Nov 20]. p. 442–50. Available from: https://www.sciencedirect.com/science/article/pii/B0123693950006242
23. Coulter JB, Birnie III DP. Assessing Tauc Plot Slope Quantification: ZnO Thin Films as a Model System. Phys Status Solidi B. 2018;255(3):1700393.
24. Prayogi S, Baqiya MA, Cahyono Y, Darminto. Optical Transmission of p-Type a-Si:H Thin Film Deposited by PECVD on ITO-Coated Glass. Mater Sci Forum. 2019;966:72–6.
25. Adachi S, Mori H, Ozaki S. Model dielectric function for amorphous semiconductors. Phys Rev B. 2002 Oct 2;66(15):153201.
26. Dingemans G, Sanden MCM van de, Kessels WMM. Influence of the Deposition Temperature on the c-Si Surface Passivation by Al2O3 Films Synthesized by ALD and PECVD. Electrochem Solid-State Lett. 2009 Dec 29;13(3):H76.
27. Prayogi S, Cahyono Y, Darminto D. Hydrogenated Amorphous Silicon Density of State Analyzed by Dielectric Function Model Derived from Ellipsometric Spectroscopy. JPSE J Phys Sci Eng. 2022 Oct 9;7(2):68–74.